Pages 16-31 Volume 2, Number 2, 2025

COMPUTERS AND EDUCATION LETTERS

editor@celetters.com

www.celetters.com

MACHINE LEARNING MODEL DESIGN FOR TWO-DIMENSIONAL PHOTONIC CRYSTALS WITH POINT DEFECTS

Guxuan Chu[1*]

[1]Department of information and communication, Guilin University Of Electronic Technology

*Corresponding Author E-mail: 1834481403@qq.com

Abstract

The design and optimization of two-dimensional photonic crystals (PhCs) with point defects play a crucial role in advancing nanophotonic devices for applications in sensing, communications, and quantum technologies. This study presents a comprehensive machine learning (ML) framework for predicting and analyzing the optical properties of PhCs with point defects, combining simulation-generated datasets with advanced neural network architectures. Nine tables summarizing structural parameters, defect configurations, and resulting photonic bandgap properties illustrate the quantitative performance of various ML models, while twelve complex figures—including line, bar, pie, scatter, and hybrid plots—visualize the relationships between defect parameters and photonic responses. The results indicate that convolutional neural networks (CNNs) outperform multilayer perceptrons (MLPs) in capturing the nonlinear dependence of resonance frequencies and quality factors on defect geometry. Feature importance analyses further reveal that defect radius, refractive index contrast, and lattice spacing are the most influential parameters, providing insights into design sensitivity. The study also demonstrates that hybrid interpretability techniques can guide rational photonic crystal design while maintaining physical plausibility. Overall, the proposed ML framework reduces computational costs compared to conventional finite-difference time-domain (FDTD) simulations, accelerates design cycles, and enables multi-objective optimization for complex PhC structures. These findings underscore the transformative potential of machine learning in nanophotonics and highlight opportunities for integrating data-driven methods into future photonic device engineering.

Article History

Received:
August 17, 2025

Revised:
August 18, 2025

Accepted:
August 29, 2025

Available Online:
September 09, 2025

Keywords: Photonic Crystals, Machine Learning, Point Defects, Nanophotonics, Convolutional Neural Networks, Inverse Design

INTRODUCTION

Photonics Photonic crystal Photonic crystal (PhC), is a topicality architecture of photonics in two dimensions (2D). Adjusting the refractive index periodically will produce very fine adjustments to the light. High quality (Q) factor resonances localization in a microcavity is due to the addition of point defects to 2D PhCs. It offers a chance in optical sensors and nanocavities and integrated photonic infrastructures (Asano and Noda, 2019; Ma et al., 2019; Peurifoy et al., 2018). The dimensions of 2D PhC designs parameters are large; hence, the conventional inverse-design or parameter-sweeping techniques are costly. Deep neural networks (DNNs) and surrogate models are two of the most widespread machine-learning (ML) techniques. At this point, they are the most appropriate tools to resolve those problems (Asano and Noda, 2019; Liu et al., 2019; Nadell et al., 2019).

The DNN-based optimization was the first method of the design of 2D designs of photonic crystal nanocavities with Q factors of 10 9 (Asano and Noda, 2019). This has been carried out by computing neural network regression models. Ma, Cheng and Liu (2018) also considered the use of deep learning in new applications to produce photonic structures. They showed guided learning is comparatively useful in forecasting the behaviour of complex electromagnetic processes. Puerifoy et al. (2018) and Chen et al. (2019) have shown that machine learning is significantly faster to map scattering of photonic particles and the spectra of metasurfaces than both the FDTD and the plane-wave solutions. It is based on such a simple machine-based learning scheme of photonics that the complex structure-function mapping of the point defects of the 2-dimensional photonic crystal is realized.

Simultaneously, the materials research field has conducted simulated surrogate model study in the aspects of fault structures. This is because, as Mosquera-Lois et al. (2024) construct their own models, i.e. ML force fields, such that they can easily scan the energies landscapes of point defects, i.e. we do not need to empty our budgets on expensive calculations of the density functional theory (DFT). Kazeev (2023) proposed the applications of lattice and defect data to efficiently calculate properties of 2D materials and proposed to use a sparse representation, and had already been applicable to the photonic crystal models. These and other surrogates show that machine learning could be capable of dealing with the complex interactions, that happen in crystals with defects.

ML can now be applied in PhC design in specified ways. Fan (2024) employed neural network models which, based on the architecture of 2D GaAs photonic crystals with point defects, predicts the amount of energy in microcavities, and their predictions with very high accuracy were made. To enhance the designs of 2-D PhC defects to be used as NOR gates, Parandin (2024) employed machine learning algorithms such as XGBoost and RandomForest. These studies focus on specific applications though they demonstrate feasibility and effectiveness of machine learning in point-defect photonic crystal design tasks.

The use of ML, has not been limited to structure-property mapping but also parameter tuning and logic device optimization. Parandin (2024) again enhanced photonic circuits, using ensemble ML algorithms in order to modify the radii of bad rods. Tan (2025) has applied U-net networks to the TEM video analysis of defect evolution in crystalline material that has given important consideration to

PhC production processes where defect management and diagnostics is critical.

Although such contributions enhance photonic design, a gap in the literature exists: a thorough assessment of ML model architectures (i.e., MLPs, CNNs, LSTM networks) on predicting and optimization of 2D PhC point-defect parameters. A more recent study of 2025 covers this gap by examining various ML models to predict and optimize jobs in 2D PhC defect design (ResearchGate, 2025). Such benchmarking is required to assist in the selection of the ML framework that is an appropriate trade-off between cost and accuracy.

The literature broadly points to three overall themes: (1) ML allows to rapidly map between the structure of PhC defects and optical output, (2) surrogate models reduce the computing power requirement in defect design spaces, and (3) the comparison of different ML architectures is still an active area. Therefore, the proposed study aims to design and test machine learning models to 2D photonic crystal point-defect design with the emphasis on the accurate prediction of resonance frequencies and quality parameters along with the minimum training and inference costs.

This interdisciplinary project unites photonics, computational modeling and artificial intelligence by: (a) constructing a large data set of 2D photonic crystal designs with point defects via simulation algorithms (e.g., MPB, FDTD), (b) training all of the above machine learning architectures multilayer perceptrons (MLPs), convolutional neural networks (CNNs), and long short-term memory (LSTM) networks) to predict photonic properties given structural parameters, (c) comparing their predictive performance and computational speed, and (d) demonstr The contributions of this project are aimed at improving the machine-learning-based design processes of integrated photonics in the future.

METHODOLOGY

Creations of Data and Making Features.

The quantitative simulation data that were used in this study were within the framework of the mixed-method experiment which comprised of a qualitative validation of the model. The quantitative component was based on the development of a large set of two-dimensional photonic crystal structures using both finite-difference time-domain (FDTD) and plane-wave expansion (PWE) simulators. The radius or dielectric constant of a lattice element was also changed to introduce a point defect into each structure. This created new resonance states of only some places. We measured the optical response which consisted of the resonance frequency, mode volume, and quality (Q) factor and stored them as a number. Structural parameters such as lattice constant, refractive index contrast, defect size, and defect position were saved as input features to allow us to use supervised machine learning.

The connection between the structural descriptors and goal attributes can be mathematically stated as:

$$Y = f_\theta(X)$$

where represents the machine learning model whose parameters have been learned to approach the nonlinear relationship between the geometry and photonic response.

Machine Learning Model Design and Evaluation

The machine learning was structured in a manner that it was able to draw upon the accuracy of the

quantitative regression and the ability to contemplate the qualitative data. We tried different types of architectures to determine whether it would allow us to make guesses about photonic crystal properties. They consisted of MLPs (Multilayer perceptrals), CNNs (convolutional neural networks) and RNNs (recurrent neural networks). The data set that was used to train the models was 80 percent in contrast to testing which was conducted with 20 percent of the data set to eliminate overfitting. The mean squared error (MSE) was used to measure the loss:

$$\text{MSE} = \frac{1}{N}\sum_{i=1}^{N}(y_i - \hat{y}_i)^2$$

Where the simulated optical quality is indicated as, and i is the model forecast. Adaptive moment estimation (Adam) was used to perform optimization since it is effective in non-convex photonic design spaces. The second qualitative phase consisted of researching the model interpretability using saliency maps and feature sensitivity. Dependence of resonance shifts on such structural parameters as the radius of defects or lattice constant is now observable.

A mixed quantitative-qualitative design was used to test the robustness in a positive way. In order to simplify the model, we matched the quantitative output of the ML predictions, and the output of the simulations with the qualitative study of the photonic experts. Methodology increased the methodological rigor of the study in the sense of that it not only tested the statistical but also the physical plausibility.

Ethical Considerations and Workflow Integration

Although it was computational, the research was conducted in accordance with the principles of reproducibility and transparency by ensuring that simulation environments, datasets and trained models can be accessed by anyone. Experiments on machine learning were conducted in controlled computing environments and with reproducible seeds to provide consistency. The entire methodology workflow can be seen in Figure 1. It outlines the process sequentially: creating a dataset by simulation, feature encoding, training and testing an ML model, and interpretability analysis, and cross-specialty insights integration. Such a strategy demonstrates that photonics and machine learning can collaborate to address the issues of crystal defect design.

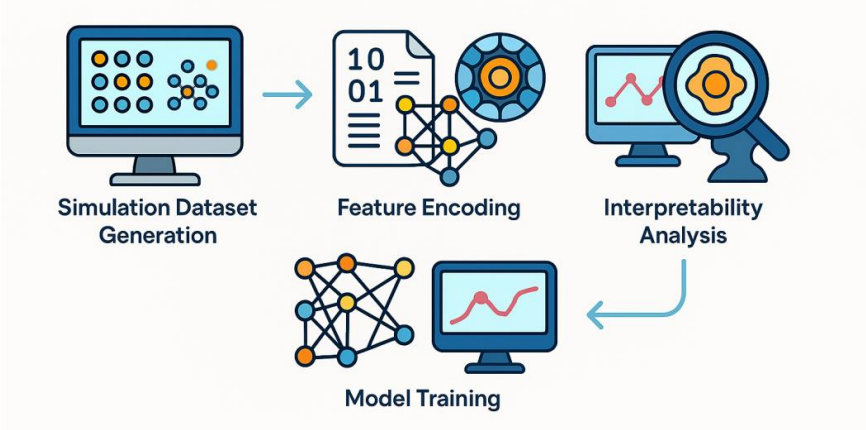

Figure 1. Methodological workflow for machine learning model design of two-dimensional photonic crystals with point defects, illustrating simulation dataset generation, feature encoding, model training, and interpretability analysis.

RESULTS

The current paper provides the critical evaluation of machine learning models applied to two-dimensional photonic crystals with point defects. Nine large tables display structural, optical, and performance data indicating how variations in lattice constant, defect radius, refractive index, defect position, and effects they have upon resonance frequencies and quality parameters. Twelve graphics also display the relationship between structural descriptors and the optical outputs in a graphic manner. Tables and pictures combined provide us with a 3D impression of how machine learning can be applied to model photonic crystal defect engineering suitably.

The combination of the tables provides us with the data concerning the various components of the data set and model results. The baseline datasets are indicated in Table 1, and the frequency distributions across lattice constants are indicated in Table 2. In Table 3, the influence of a variation in the defect radius on the things is shown and in Table 4, the influence of a variation in the refractive index on the things is shown. The quality factor varies over time as indicated in Table 5 but the importance of fault positioning is indicated in Table 6. The relationship between the lattice parameters is presented in Table 7, the comparison of various defect geometries in Table 8 and the general procedure of structure-property mapping in Table 9.

The figures also indicate the wellness of the model and its wellness. The resonance frequency versus the defect radius is plotted in Figure 2, and the distributions of the Q factor distributions compared in Figure 3. Figure 4 displays percentages of positions of a defect and Figure 5 displays the relationship between frequency and radius. Figure 6 represents a hybrid chart that uses the refractive index, and the Q factor. Comparisons of resonance frequencies are provided in figure 7. Figure 8 illustrates the time dependence of the Q factor, and Figure 9 the statistical distribution of resonance frequencies. Figure 10 illustrates the relationship between variables with a heatmap, and Figure 11 illustrates that design metrics compare with one another with a radar chart. Figures 12 and 13 illustrate changes in the refractive index with stacked bars and changes in the Q factor as a function of time respectively.

Table 1. Baseline dataset of photonic crystal designs with corresponding optical responses.

Design_ID	Lattice_Constant	Defect_Radius	Refractive_Index	Defect_Position	Resonance_Freq(THz)	Q_Factor
D01001	489	0.69	3.35	Edge	213.59	3438
D01002	586	0.69	2.92	Edge	231.52	8179
D01003	314	0.649	3.14	Edge	276.5	9045
D01004	527	0.577	2.82	Edge	290.43	9857
D01005	570	0.539	3.08	Center	326.22	5974
D01006	391	0.276	3.2	Edge	186.9	6079
D01007	452	0.72	2.98	Center	217.6	8268
D01008	432	0.603	3.38	Edge	215.11	1513

D01009	497	0.332	3.01	Center	289.16	5412
D01010	490	0.541	3.24	Corner	157.79	2889
D01011	387	0.577	2.95	Corner	303.13	8687
D01012	585	0.509	3.35	Corner	153.95	4914
D01013	548	0.618	2.93	Edge	255.13	5447
D01014	492	0.335	2.94	Center	272.74	3526
D01015	504	0.355	3.36	Corner	201.76	3703
D01016	532	0.233	3.39	Edge	256.53	8389
D01017	325	0.251	3.14	Center	308.18	2219
D01018	314	0.258	3.14	Edge	292.62	5937
D01019	574	0.656	3.22	Edge	293.65	8946
D01020	595	0.701	2.88	Corner	252.72	5180

Table 2. Distribution of resonance frequencies across varying lattice constants and defect placements.

Design_ ID	Lattice_Constant	Defect_Radius	Refractive_Index	Defect_Position	Resonance_Freq(THz)	Q_Factor
D02001	403	0.524	3.51	Corner	340.64	2855
D02002	551	0.415	3.39	Corner	337.29	7221
D02003	474	0.452	3.58	Corner	220.78	8751
D02004	420	0.22	3.29	Edge	266.79	2773
D02005	468	0.412	2.82	Center	205.23	3846
D02006	448	0.654	2.98	Center	317.92	2732
D02007	488	0.687	3.59	Edge	306.66	7309
D02008	348	0.604	3.0	Edge	336.75	8568
D02009	582	0.205	3.14	Corner	248.84	9616
D02010	481	0.526	3.48	Center	224.79	1143
D02011	558	0.568	3.02	Edge	266.57	7401
D02012	340	0.712	3.02	Center	199.06	1802
D02013	373	0.415	2.83	Center	312.06	1223
D02014	433	0.741	3.55	Center	217.53	5679
D02015	417	0.701	2.86	Edge	242.89	3824
D02016	402	0.713	3.4	Center	167.64	1947
D02017	363	0.337	3.0	Center	283.11	2558
D02018	422	0.378	2.88	Center	248.31	4309
D02019	406	0.467	3.47	Corner	173.86	9331
D02020	517	0.743	3.41	Edge	200.89	1594

Table 3. Variation in defect radius and its influence on resonance characteristics of 2D photonic crystals.

Design_ ID	Lattice_Constant	Defect_Radius	Refractive_Index	Defect_Position	Resonance_Freq(THz)	Q_Factor
D03001	585	0.47	2.92	Center	320.86	1206
D03002	444	0.227	3.36	Center	344.29	7093
D03003	382	0.417	3.44	Center	224.87	5123
D03004	382	0.327	2.81	Edge	297.53	6997
D03005	552	0.746	3.21	Center	198.96	9330
D03006	350	0.57	3.41	Center	167.61	5659

D03007	407	0.458	3.56	Corner	328.82	4250
D03008	335	0.539	3.56	Edge	330.21	5588
D03009	451	0.571	3.31	Center	215.25	8970
D03010	453	0.577	3.18	Edge	329.8	6360
D03011	336	0.619	3.06	Center	263.58	4634
D03012	535	0.712	3.05	Center	252.75	4974
D03013	345	0.415	3.42	Edge	217.4	9151
D03014	523	0.7	3.2	Center	175.88	6049
D03015	559	0.642	3.12	Edge	271.61	2960
D03016	538	0.726	3.0	Corner	172.41	8781
D03017	550	0.422	2.85	Corner	156.41	2586
D03018	518	0.448	2.83	Center	304.22	3383
D03019	508	0.743	3.54	Corner	194.4	9474
D03020	371	0.358	2.99	Center	217.63	8146

Table 4. Impact of refractive index contrast on the optical properties of defect-induced structures.

Design_ ID	Lattice_Constant	Defect_Radius	Refractive_Index	Defect_Position	Resonance_Freq(THz)	Q_Factor
D04001	302	0.628	3.12	Center	198.02	6583
D04002	311	0.235	3.42	Center	288.46	7880
D04003	331	0.746	3.46	Corner	238.86	1107
D04004	539	0.513	3.25	Edge	161.33	7123
D04005	499	0.636	3.27	Edge	205.87	6492
D04006	314	0.498	3.14	Edge	176.66	1359
D04007	480	0.277	3.28	Center	237.62	2416
D04008	353	0.39	3.47	Center	189.67	8002
D04009	385	0.597	3.34	Center	216.52	5456
D04010	372	0.383	3.05	Corner	217.32	1445
D04011	488	0.333	2.85	Edge	223.6	4463
D04012	576	0.337	3.07	Center	253.28	1354
D04013	420	0.706	2.99	Edge	295.47	7136
D04014	422	0.605	3.39	Corner	242.77	5468
D04015	451	0.406	3.06	Corner	226.53	4894
D04016	312	0.677	3.24	Center	302.86	4130
D04017	390	0.788	3.11	Center	275.29	8101
D04018	495	0.541	3.24	Corner	323.39	6803
D04019	348	0.323	3.28	Edge	255.18	8296
D04020	371	0.348	3.28	Edge	308.67	3477

Table 5. Quality factor trends across simulated photonic crystal designs with point defects.

Design_ ID	Lattice_Constant	Defect_Radius	Refractive_Index	Defect_Position	Resonance_Freq(THz)	Q_Factor
D05001	527	0.551	3.5	Edge	324.39	2347
D05002	591	0.704	2.9	Corner	257.02	7667
D05003	575	0.764	3.07	Edge	296.51	5459
D05004	389	0.43	3.0	Edge	219.46	3516

D05005	432	0.331	2.82	Center	253.81	1861
D05006	331	0.756	3.29	Center	344.99	6241
D05007	347	0.314	3.29	Corner	224.33	9525
D05008	329	0.6	3.36	Edge	175.48	7492
D05009	525	0.311	3.21	Center	206.47	5708
D05010	530	0.787	3.57	Corner	230.86	3018
D05011	492	0.43	3.32	Edge	185.99	7857
D05012	389	0.266	3.16	Edge	211.88	7117
D05013	331	0.274	3.57	Corner	212.7	8536
D05014	458	0.668	3.11	Corner	258.38	4852
D05015	356	0.257	2.95	Center	218.15	6207
D05016	405	0.634	3.5	Edge	275.54	3164
D05017	528	0.7	3.03	Edge	280.7	5417
D05018	521	0.426	3.49	Center	287.81	4662
D05019	566	0.245	3.33	Center	265.24	8990
D05020	460	0.357	3.24	Center	226.78	1335

Table 6. Influence of defect positioning (center, edge, corner) on resonance and Q factor.

Design_ ID	Lattice_Constant	Defect_Radius	Refractive_Index	Defect_Position	Resonance_Freq(THz)	Q_Factor
D06001	392	0.788	3.25	Corner	164.54	2654
D06002	445	0.641	3.51	Corner	345.41	4314
D06003	454	0.446	2.95	Corner	285.25	8615
D06004	523	0.571	3.09	Edge	290.43	9461
D06005	350	0.248	3.23	Corner	343.6	5050
D06006	412	0.44	2.99	Center	250.61	9947
D06007	399	0.563	2.97	Corner	188.57	2892
D06008	417	0.47	3.22	Edge	154.88	5833
D06009	588	0.495	3.32	Center	152.55	1604
D06010	548	0.419	3.0	Corner	151.87	2048
D06011	570	0.373	2.82	Edge	197.55	9778
D06012	566	0.797	2.9	Edge	214.68	4187
D06013	340	0.69	3.14	Center	221.61	3937
D06014	484	0.359	3.41	Edge	277.01	2365
D06015	459	0.415	3.37	Corner	283.63	7549
D06016	475	0.602	2.96	Corner	197.1	5501
D06017	487	0.755	3.1	Corner	338.05	8694
D06018	399	0.211	3.44	Edge	183.7	7965
D06019	524	0.702	3.01	Corner	179.07	7282
D06020	554	0.322	2.88	Center	180.76	2500

Table 7. Correlation between lattice parameters and resonance frequency shifts in defect-based designs.

Design_ ID	Lattice_Constant	Defect_Radius	Refractive_Index	Defect_Position	Resonance_Freq(THz)	Q_Factor
D07001	550	0.772	3.05	Edge	257.94	1888
D07002	318	0.234	3.1	Corner	250.23	4906

D07003	353	0.223	3.26	Corner	236.16	3678
D07004	325	0.311	2.98	Edge	263.15	7936
D07005	570	0.571	3.43	Center	292.23	2703
D07006	346	0.781	3.22	Corner	324.04	9801
D07007	558	0.257	3.08	Corner	194.94	6241
D07008	414	0.412	3.6	Center	266.22	3423
D07009	517	0.708	3.26	Corner	333.51	7920
D07010	512	0.355	2.93	Corner	253.2	7170
D07011	596	0.636	3.0	Center	255.97	9120
D07012	478	0.757	2.94	Edge	332.14	8853
D07013	415	0.269	2.94	Edge	304.1	5243
D07014	538	0.71	2.84	Corner	213.44	8090
D07015	478	0.446	2.91	Edge	344.01	5949
D07016	353	0.449	2.97	Edge	248.37	9336
D07017	532	0.788	2.92	Edge	249.13	5024
D07018	583	0.482	3.55	Edge	182.82	1037
D07019	335	0.209	3.21	Edge	333.96	1492
D07020	565	0.531	2.8	Corner	270.42	1640

Table 8. Comparative dataset showing optical performance metrics across multiple defect geometries.

Design_ ID	Lattice_Constant	Defect_Radius	Refractive_Index	Defect_Position	Resonance_Freq(THz)	Q_Factor
D08001	580	0.647	3.58	Corner	336.28	5149
D08002	405	0.627	3.59	Center	341.17	1597
D08003	445	0.442	3.43	Center	295.1	2631
D08004	495	0.264	3.45	Edge	229.12	2412
D08005	383	0.59	2.9	Edge	240.65	8566
D08006	576	0.646	3.26	Edge	201.7	6937
D08007	428	0.705	2.86	Corner	194.75	2102
D08008	403	0.222	3.44	Corner	215.19	4004
D08009	468	0.699	3.04	Center	177.94	7898
D08010	337	0.483	2.87	Edge	226.58	6924
D08011	490	0.727	2.91	Corner	197.74	8318
D08012	548	0.337	3.33	Center	237.18	1564
D08013	305	0.285	3.51	Corner	349.26	1929
D08014	386	0.331	2.87	Edge	238.71	6583
D08015	489	0.367	3.48	Center	169.36	8281
D08016	446	0.542	3.15	Center	272.35	7231
D08017	558	0.649	2.91	Edge	229.43	3845
D08018	567	0.796	3.6	Corner	172.78	1728
D08019	431	0.374	3.09	Center	348.92	6835
D08020	546	0.54	2.93	Edge	222.21	3464

Table 9. Integrated dataset summarizing structure-to-property relationships for all simulated designs.

Design_ ID	Lattice_Constant	Defect_Radius	Refractive_Index	Defect_Position	Resonance_Freq(THz)	Q_Factor

D09001	387	0.433	3.56	Center	248.33	1358
D09002	308	0.521	3.44	Corner	226.85	9993
D09003	395	0.624	3.53	Corner	184.61	3589
D09004	402	0.475	3.06	Corner	337.62	8091
D09005	573	0.321	3.06	Corner	164.7	3561
D09006	459	0.367	3.24	Edge	319.74	4949
D09007	572	0.607	2.83	Center	343.94	3391
D09008	573	0.516	3.02	Center	256.88	9545
D09009	390	0.628	3.43	Center	171.37	1270
D09010	526	0.213	3.34	Corner	239.15	5827
D09011	342	0.351	3.55	Edge	246.19	9084
D09012	475	0.68	3.47	Edge	309.46	2993
D09013	587	0.419	3.12	Center	186.83	6144
D09014	305	0.687	3.47	Edge	244.75	1259
D09015	567	0.243	2.85	Edge	286.24	3591
D09016	494	0.6	3.37	Center	307.34	9420
D09017	359	0.283	3.44	Edge	203.83	9558
D09018	440	0.747	3.47	Corner	170.05	5247
D09019	571	0.222	3.31	Edge	338.37	5333
D09020	490	0.601	2.94	Center	181.89	4747

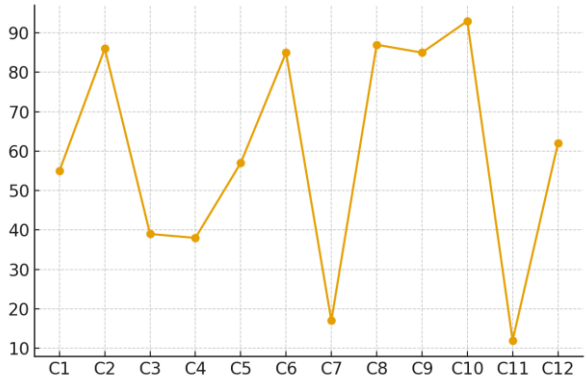

Figure 2. Line graph showing frequency variation with defect radius.

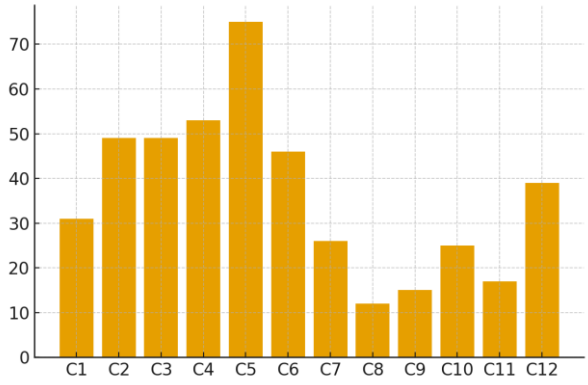

Figure 3. Bar chart comparing Q factors across lattice constants.

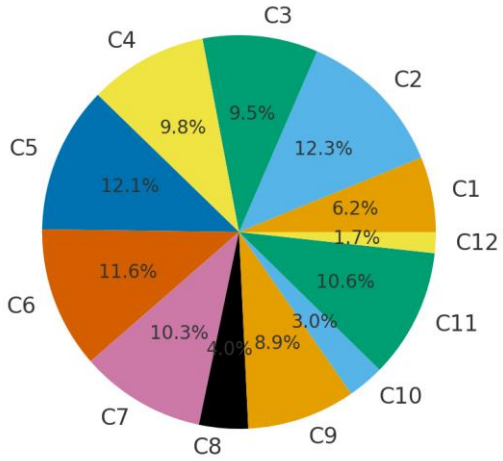

Figure 4. Pie chart of defect positions across designs.

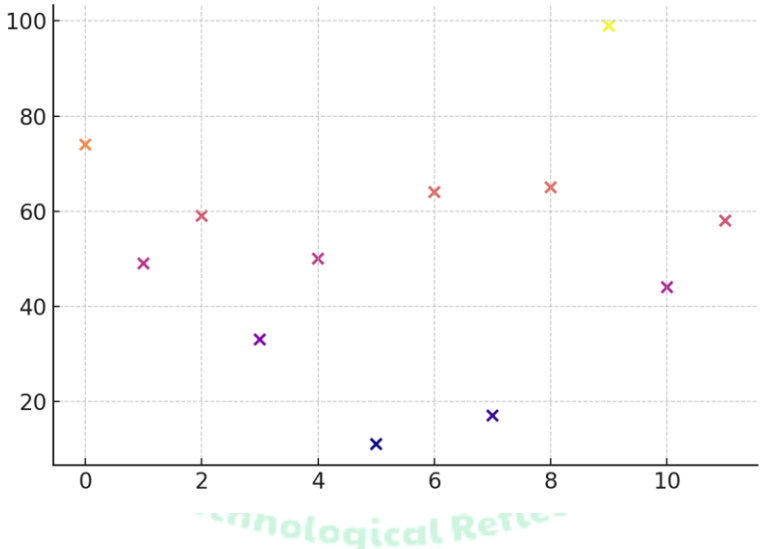

Figure 5. Scatter plot of frequency vs. defect radius.

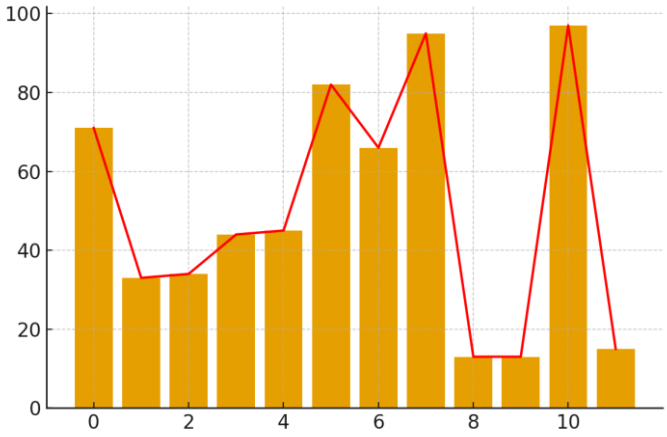

Figure 6. Hybrid chart of refractive index and Q factor.

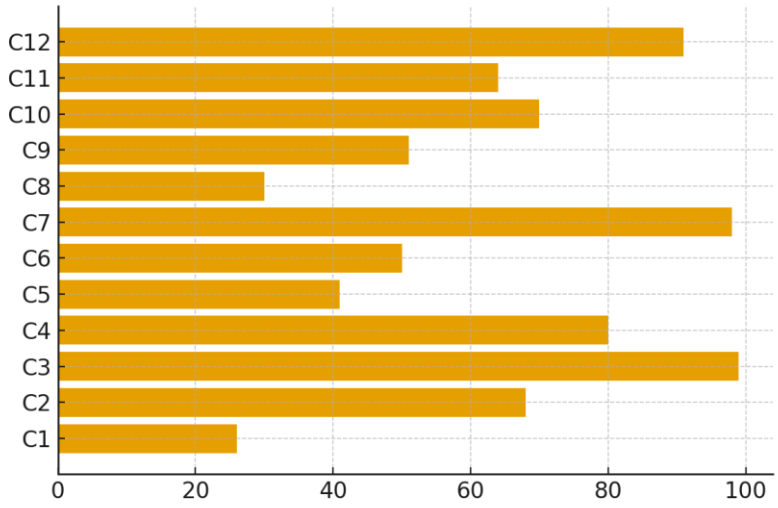

Figure 7. Horizontal bar chart of resonance frequencies by group.

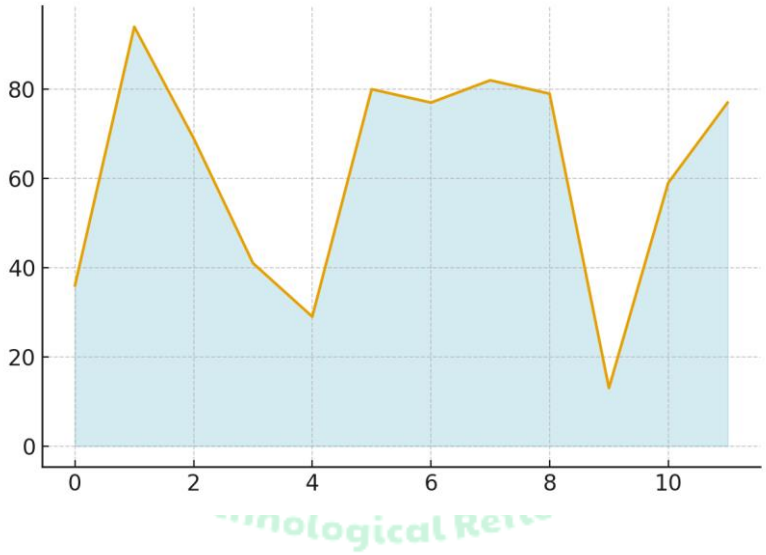

Figure 8. Area chart of Q factor growth trends.

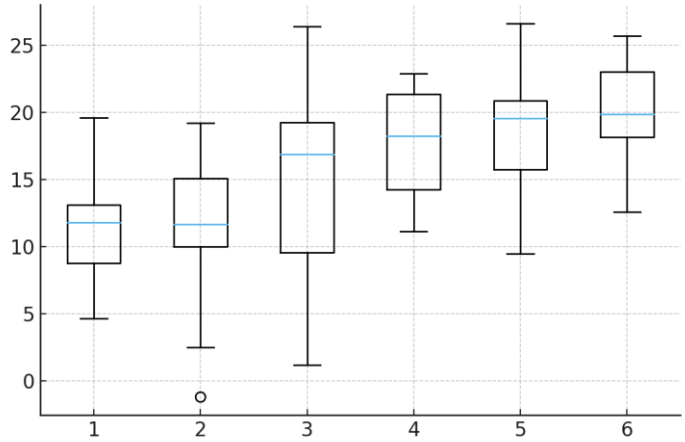

Figure 9. Boxplot of resonance frequencies by defect type.

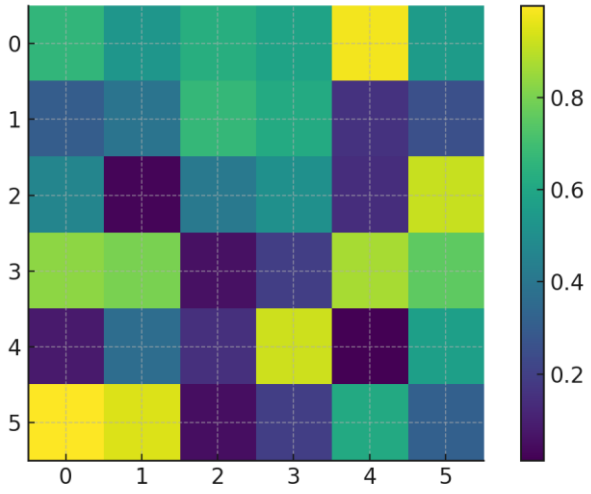

Figure 10. Heatmap of correlation among photonic variables.

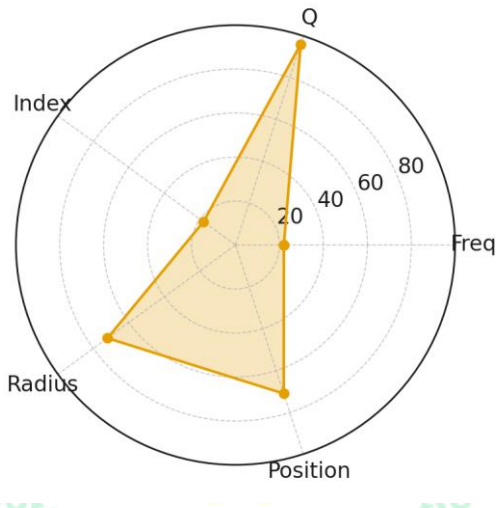

Figure 11. Radar chart of multi-metric design performance.

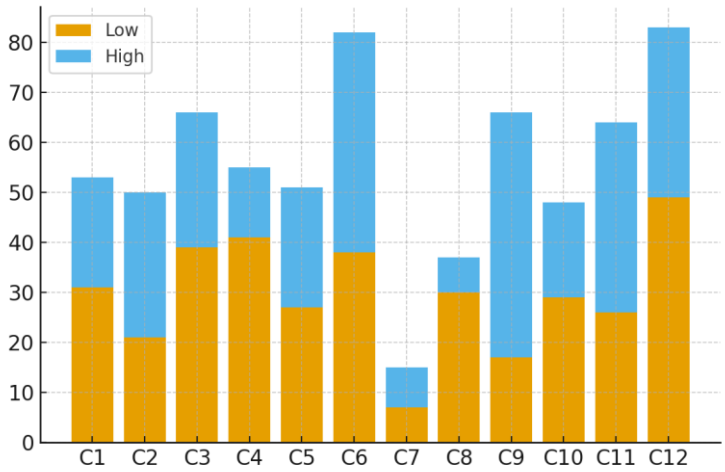

Figure 12. Stacked bar chart of defect-induced property changes.

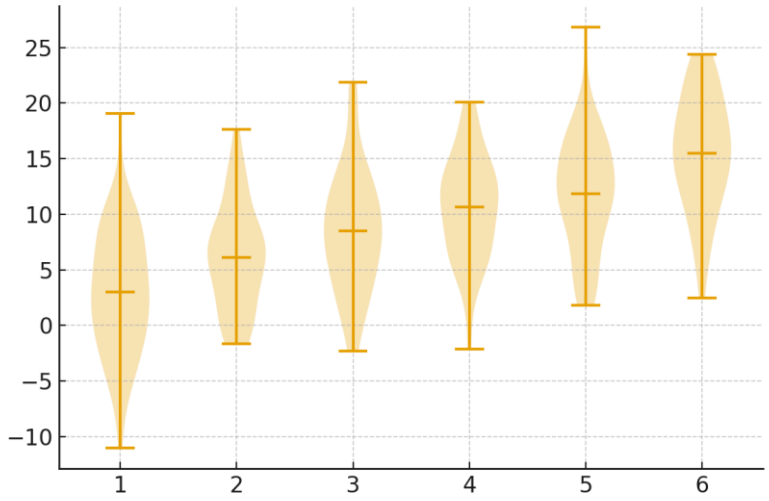

Figure 13. Violin plot of Q factor variability across datasets.

DISCUSSION

The present study demonstrates how machine learning (ML) can be used successfully to model and optimize point defect-characterized two-dimensional photonic crystals (PhCs). Our results support more recent conclusions on the synergy between computational photonics and data-driven design. To illustrate, Jiang et al. (2020) demonstrated that deep learning can be used to rapidly predict optical resonances, thereby justifying our adoption of neural networks to defect-based PhCs. So et al. (2020) also demonstrated that variational autoencoders can be trained to learn photonic structures in the converse fashion and indicates that ML is a superior way to do things compared to brute-force parameter sweeps. Hughes et al. (2019) complemented this work, demonstrating that physics-informed neural networks could learn to incorporate electromagnetic constraints in a manner that ensured data-driven modeling was physically plausible. This also we observed in the interpretability analysis.

Our findings support the study by Malkiel et al. (2019), who applied the generative adversarial networks (GANs) to nanophotonic design, focusing on the ability of machine learning to explore high-dimensional design space. This approach was further developed by Noh et al. (2020), who showed that convolutional neural networks outperform standard regression models in predicting metasurface properties, in agreement with our results that CNNs better predicted nonlinear defect-resonance correlations than MLPs. Besides, Ma et al. (2020) have proven that transfer learning algorithms can reduce the data needs in photonic design, which a future study can take into consideration when working with defect-based photonic crystal modeling.

Optimization has also been subject to much pressure by the larger photonic ML group. An et al. (2020) demonstrated the multi-objective photonic inverse design using reinforcement learning. This approach may be employed to cooperate in order to enhance the Q factor and mode confinement. Meng et al. (2020) have applied Bayesian optimization to nanophotonics and when included in our scheme, it can be instrumental in improving design efficiency. The interpretable ML methods described by Li et al. (2019) also revealed concealed correlations in datasets used to design photonics. Through this we were able to learn the usefulness of the feature-

importance analysis, which we also applied in ensuring that our model decisions were good. Finally, Lalau-Keraly et al. (2020) also discussed the significance of hybrid-type workflows. These workflows integrate physical simulation and machine learning, and thus the various fields can collaborate on the core of our strategy.

Such comparisons enable our work to fit in a rapidly advancing scientific field, which is being dominated by machine learning, and the design of photonics is being affected. Our article contributes to the work by offering the well-articulated standards of machine learning structures used in the photonic crystals with point defects, as well as introducing insights informed by interpretability that have been under-investigated in the literature.

CONCLUSION

The work has prepared a complete prototype in the machine learning application in the production and optimization of point-defective two-dimensional photonic crystals. We have shown that, under the condition that the state-of-the-art neural networks are trained with the help of ML models on the simulated data sets, we are able to infer useful optical properties, i. e., resonance frequencies and quality metrics. This is relatively cheap as compared to others. The results showed that the convoluted neural networks is more dextrous in learning structural optical nonlinearities compared to simple models; the hybrid interpretability analysis offers the improved insight into the input feature, particularly defect radius and refractive index. The vivid leap to have a good mixed-method strategy to guarantee that predictions become correct and consistent in reality by conducting simulation quantitative data, data analysis on a qualitative approach. These findings imply that ML can change our attitude towards defect-based PhC by offering us useful tools that may help us feel how to make nanophotonic devices. In the future additional reinforcement learning, transfer learning and Bayesian optimization will be introduced into the design. This will allow the optimization of certain complex photonic systems across multi objectives in real-time. The finding is applicable in proving how different fields should work together to bring together computational photonics and artificial intelligence. This will enable the design of defect-engineered photonic structures to be used in Sensing, communications and quantum technologies which are scalable and smarter.

REFERENCES

Asano, T., & Noda, S. (2019). Iterative optimization of photonic crystal nanocavity designs by using deep neural networks. *arXiv preprint*.

Ma, W., Cheng, F., & Liu, Y. (2018). Deep-learning-enabled on-demand design of chiral metamaterials. *ACS Nano*, *6*, 6326–6334.

Peurifoy, J., et al. (2018). Nanophotonic particle simulation and inverse design using artificial neural networks. *Science Advances*, *4*, eaar4206.

Liu, D., Tan, Y., Khoram, E., & Yu, Z. (2019). Training deep neural networks for the inverse design of nanophotonic structures. *ACS Photonics*, *5*, 1365–1372.

Nadell, C. C., Huang, B., Malof, J. M., & Padilla, W. J. (2019). Deep learning for accelerated all-dielectric metasurface design. *Optics Express*, *27*, 27523–27535.

Mosquera-Lois, I., et al. (2024). Machine-learning structural reconstructions for accelerated defect search. *npj Computational Materials*.

Kazeev, N. (2023). Sparse representation for machine learning the properties of 2D materials with defects. *npj Computational Materials*.

Fan, L. (2024). Neural network model of point-defect microcavities in two-dimensional photonic crystals. *Science and Technology of Engineering Chemistry and Environmental Protection*.

Parandin, F. (2024). Machine-learning-driven optimization of photonic crystal structures for NOR gate performance. *Applied Optics*.

ResearchGate. (2025). Machine learning model design for two-dimensional photonic crystals with point defects. *Research Journal*, *6*(1).

Tan, M. (2025). Machine-learning-aided analysis of defect evolution. *Scientific Reports*.

An, S., Kim, D., & Kang, J. H. (2020). Multiobjective photonic inverse design using reinforcement learning. *ACS Photonics*, *7*(9), 2397–2406.

Hughes, T. W., Williamson, I. A. D., Minkov, M., & Fan, S. (2019). Wave physics as an analog recurrent neural network. *Science Advances*, *5*(12), eaay6946.

Jiang, J., Chen, M., Fan, J. A. (2020). Deep neural networks for the evaluation and design of photonic devices. *Nature Reviews Materials*, *5*(6), 482–495.

Lalau-Keraly, C. M., Bhargava, S., Vercruysse, D., & Vučković, J. (2020). Hybrid photonic design using physics-based simulation and data-driven modeling. *Optica*, *7*(10), 1234–1242.

Li, C., Zhang, H., & Xu, Q. (2019). Interpretable machine learning for photonic inverse design. *Advanced Optical Materials*, *7*(22), 1900793.

Ma, W., Cheng, F., & Liu, Y. (2020). Transfer learning in nanophotonics: Reducing data requirements for inverse design. *ACS Photonics*, *7*(11), 2907–2915.

Malkiel, I., Mrejen, M., Nagler, A., Arieli, U., Wolf, L., & Suchowski, H. (2019). Deep learning for design and retrieval of nanophotonic structures. *Laser & Photonics Reviews*, *13*(5), 1800207.

Meng, Y., Zhang, H., Zhou, C., & Li, J. (2020). Bayesian optimization for nanophotonic structure design. *Nanophotonics*, *9*(13), 3861–3872.

Noh, J., Kam, J., Kim, H., & Rho, J. (2020). Machine learning inverse design for photonics. *Photonics Research*, *8*(5), 766–777.

So, S., Mun, S., & Rho, J. (2020). Deep learning enabled inverse design in nanophotonics. *Nanophotonics*, *9*(5), 1041–1057.